RESEARCH ARTICLE | NOVEMBER 02 2020

Quantum accurate SNAP carbon potential for MD shock simulations

Jonathan T. Willman; Ashley S. Williams; Kien Nguyen-Cong; Aidan P. Thompson; Mitchell A. Wood; Anatoly B. Belonoshko; Ivan I. Oleynik

AIP Conf. Proc. 2272, 070055 (2020)
https://doi.org/10.1063/12.0000881

Quantum Accurate SNAP Carbon Potential for MD Shock Simulations

Jonathan T. Willman,[1] Ashley S. Williams,[1] Kien Nguyen-Cong,[1] Aidan P. Thompson,[2] Mitchell A. Wood,[2] Anatoly B. Belonoshko,[3] and Ivan I. Oleynik[1, a)]

[1)]*Department of Physics, University of South Florida, 4204 E Fowler Ave, Tampa FL. 33620, USA*
[2)]*Sandia National Laboratories, Albuquerque NM. 87185 USA*
[3)]*Department of Physics, Royal Institute of Technology (KTH), Albanova 10691 Stockholm, Sweden*

[a)]*Corresponding author: oleynik@usf.edu*

Abstract. We present a new quantum accurate Spectral Neighbor Analysis Potential (SNAP) machine-learning potential for simulating carbon under extreme conditions of dynamic compression (pressures up to 1 TPa and temperatures up to 10,000 K). The development of SNAP potential involves (1) the generation of the training database comprised of the consistent and meaningful set of first-principles DFT (Density Functional Theory) data for carbon materials at high pressure and temperature; (2) the robust and physically guided training of the SNAP parameters on first-principles data involving statistical data analysis; and (3) the validation of the SNAP potential in MD simulations of carbon at high PT conditions. The excellent performance of quadratic SNAP potential is demonstrated by simulating the radial distribution functions at high pressure-temperature conditions and melt curve of diamond, which were found in good agreement with DFT.

INTRODUCTION

The ability of molecular dynamics (MD) to realistically simulate the high-strain-rate shock physics is critically dependent on the availability of high fidelity interatomic potentials capable of capturing the major physics of materials response to high temperatures and pressures. The lack of good quality interatomic potentials has been a stumbling block towards predictive MD shock simulations of shock compression of diamond [1, 2, 3, 4]. Although recent activities in developing machine learning interatomic potentials provide a promise of capturing complex material properties [5, 6, 7, 8], such potentials have not been applied for simulation of materials at extreme conditions. In this work we make the first step in this direction and present in this paper the preliminary results on development of the Spectral Neighbor Analysis Potential (SNAP) potential [7] for MD simulations of carbon.

DESCRIPTION OF SNAP

The SNAP formalism is described in Refs [7, 8] but for completeness it is briefly discussed here as well.

The potential energy of the system of N atoms is represented as a sum of SNAP energies for each atom i

$$E(\{\mathbf{r}_N\}) = \sum_{i=1}^{N} E^i_{SNAP}, \tag{1}$$

where $\{\mathbf{r}_N\}$ is the $3N$-dimensional vector of cartesian coordinates of the system of N atoms. The SNAP energy of the atom is written as a quadratic function of bispectrum coefficients $\mathbf{B}^i$

$$E^i_{SNAP}(\{\mathbf{r}_N\}) = \boldsymbol{\beta}\mathbf{B}^i + \frac{1}{2}\left(\mathbf{B}^i\right)^T \cdot \boldsymbol{\alpha} \cdot \mathbf{B}^i \tag{2}$$

Being a set of the expansion coefficients of the local atomic density ρ_i, consisting of the sum of contributions of neighbor atoms j, over hyperspherical harmonics, the vector of bispectrum coefficients $\mathbf{B}^i$ uniquely characterizes the atomic environment around the atom i, and is therefore, considered as a set of descriptors. The potential energy is expressed as a linear function of unknown coefficients $\boldsymbol{\alpha}$ and $\boldsymbol{\beta}$, which are effectively determined by mapping the descriptor space $\mathbf{B}^i$ to the training database using methods of linear regression [7].

Shock Compression of Condensed Matter - 2019
AIP Conf. Proc. 2272, 070055-1–070055-5; https://doi.org/10.1063/12.0000881
Published by AIP Publishing. 978-0-7354-4000-5/$30.00

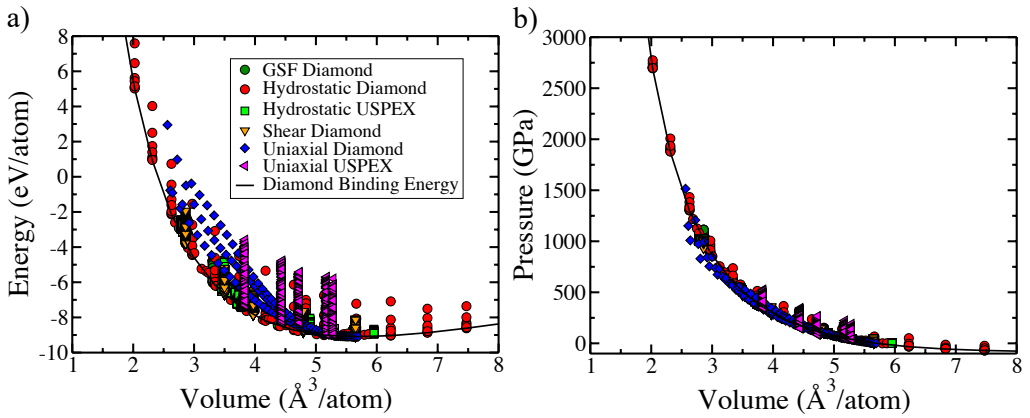

FIGURE 1. a) Energy versus volume and b) pressure versus volume for all 5,000 structures included in SNAP training database.

There are two classes of SNAPs: linear SNAP retains only the first linear term in (2) and is defined by set of unknown coefficients β, whereas quadratic SNAP keeps both linear and quadratic terms and is defined by two sets of unknown coefficients α and β. Being less accurate, the linear SNAP is computationally inexpensive compared to more accurate but more computationally demanding quadratic SNAP. The computational cost as well as accuracy of both linear and quadratic SNAPs is determined by the number of bispectrum coefficients $\mathbf{B}^i$ calculated for each atom i, which is in turn specified by the maximum order J_{max} of the hyperspherical harmonics in the expansion of the atomic density ρ_i.

The linear SNAP displays a saturation in accuracy whereas the quadratic SNAP systematically improves its accuracy upon increasing J_{max}. Being an order of magnitude more accurate, the quadratic SNAP is only twice as slow as linear SNAP [8]. Both linear and quadratic SNAPs are implemented in LAMMPS MD software package [9].

RESULTS

The first step of SNAP development for carbon materials involves the generation of a training database comprised of the consistent and meaningful set of first-principles DFT data for various carbon structures at both ambient conditions and high pressures and temperatures most relevant to shock wave experiments. These include diamond uniaxial and hydrostatic compressions, which were heavily sampled up to 1TPa. Diamond defects such as mono and di-vacancies, generalized stacking faults and shear deformations were also included. Additional metastable carbon phases were generated by performing two types of evolutionary crystal structure prediction searches using USPEX method [10, 11, 12]. The first type of search consisted of fixed hydrostatic pressure searches performed at 100 GPa, 500 GPa and 1 TPa. The second type consisted of fixed volume searches corresponding to the uniaxial compression of diamond along the <100>, <110> and <111> direction. The c-lattice parameter of the crystals generated in the search is held fixed in order to sample the associated longitudinal stress of 100, 300, and 500 GPa in each crystal. Energies, forces and the stress tensor of each system were calculated by DFT using VASP ab-inio software [13]. The expansive range of atomic energies and volumes of structures included in our database can be observed in Fig 1.

To introduce non-zero forces into database configurations, random displacements of atomic positions were generated by running first-principles DFT MD in NVE micro-canonical ensemble with temperatures ranging from 300K to 20,000K. From each simulation, ten uncorrelated frames were chosen from the MD trajectory. Static (0 Kelvin) calculations of energies, forces and stresses were then made on each structure using VASP.

Once the first-principles training database is constructed, the SNAP coefficients α and β are determined using linear regression by matching the SNAP energies, atomic forces and stress tensor components for every structure of the training database to those calculated by DFT. We found that linear SNAP displays subpar accuracy in describing such a diverse set of structures within the extreme range of pressures and temperatures covered. Therefore, we employed quadratic SNAP in this work, which provides much better description of these systems and conditions. To ensure a good quality of the potential's predictions, the number of descriptors has been carefully chosen to include 55 bispectrum descriptors, which results in the same number of linear α and $1,540$ quadratic β coefficients.

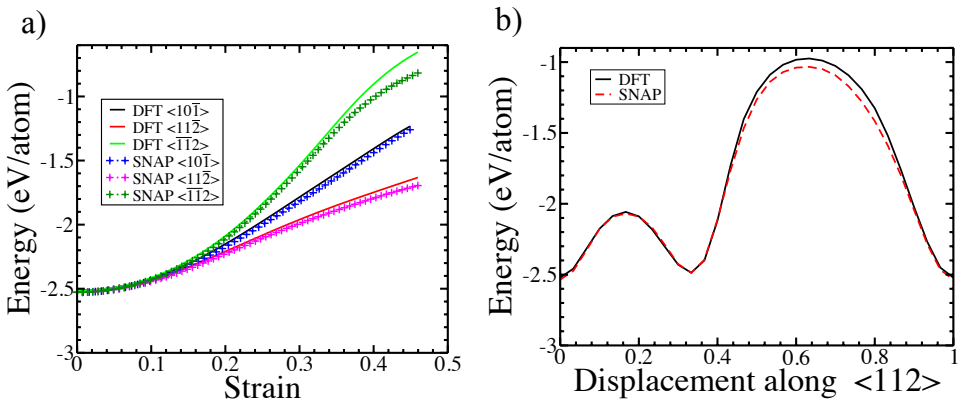

FIGURE 2. Accuracy of SNAP compared to DFT: (a) energy vs strain for (111) shear deformations of diamond along $< 10\bar{1} >$, $< 11\bar{2} >$, $< \bar{1}\bar{1}2 >$ directions; (b) energy vs displacement curve for (111) generalized stacking fault energy profile along $< 112 >$ direction.

To demonstrate a high accuracy of the fit, we calculate the dependence of the energy on the shear strain upon application of the shear to (111) planes of diamond along several directions (Fig. 2a) and generalized stacking fault energy profile for the (111) slip plane along <112> direction (Fig. 2b). Both cases display a very good agreement between SNAP and DFT, which demonstrates an excellent quality of the SNAP training.

SNAP VALIDATION

To demonstrate SNAP's ability to make reliable predictions of the properties which were not included in SNAP training database, we concentrate on physically meaningful calculations, which can be performed using both SNAP and DFT MD. They include MD simulations of radial distribution function of different solid and liquid carbon phases at multiple pressures and temperatures, and the melting line of diamond within a wide range of pressures.

The RDFs were obtained from NVE MD simulations of diamond and liquid phases at corresponding pressures and temperatures of their stability and compared with those calculated using DFT MD, see Fig. 3. The pressures and temperatures used are (23 GPa, 3884 K) -diamond, (90 GPa, 5867 K) - liquid carbon, (450 GPa, 7013 K) -diamond, and (457 GPa, 6922 K) - liquid carbon. In all cases SNAP RDFs are in an excellent agreement with those obtained by DFT.

Another stringent test is simulation of diamond (T,P) melting line. We employ two complimentary methods for melting line calculations: (1) two-phase method, and (2) so-called Z-method. Fig. 4 shows results of SNAP melting line calculations by both methods as well as other DFT simulations by Benedict *et. al* [14], and our own independent DFT calculations by Nguyen Cong [15]. Although the Z-method, which involves a series of NVE simulations at elevated temperatures to overheat the crystal until it transforms to a liquid state, does not agree well with more precise two-phase method calculations, the final (P,T) states for each SNAP MD run are in a very good agreement with DFT. More importantly, two-phase SNAP simulation of diamond melt line agrees well with our own DFT simulations as well as with previous results by Benedict *et. al* [14], which demonstrates an encouraging level of transferability of SNAP beyond its training database, thus promising to deliver high quality results in future MD shock simulations.

CONCLUSION

We have demonstrated the potential of quadratic SNAP to describe very complex physics and chemistry of carbon at extreme conditions of pressures (up to 1 TPa) and temperatures (up to 10,000 K). A comprehensive SNAP fitting database of very accurate DFT calculations of various carbon structures has been utilized to determine SNAP parameters, It has been demonstrated that SNAP possesses an abundance of flexibility and a high level of accuracy to represent an expansive energy and pressure landscape represented in our database by carbon structures at extreme

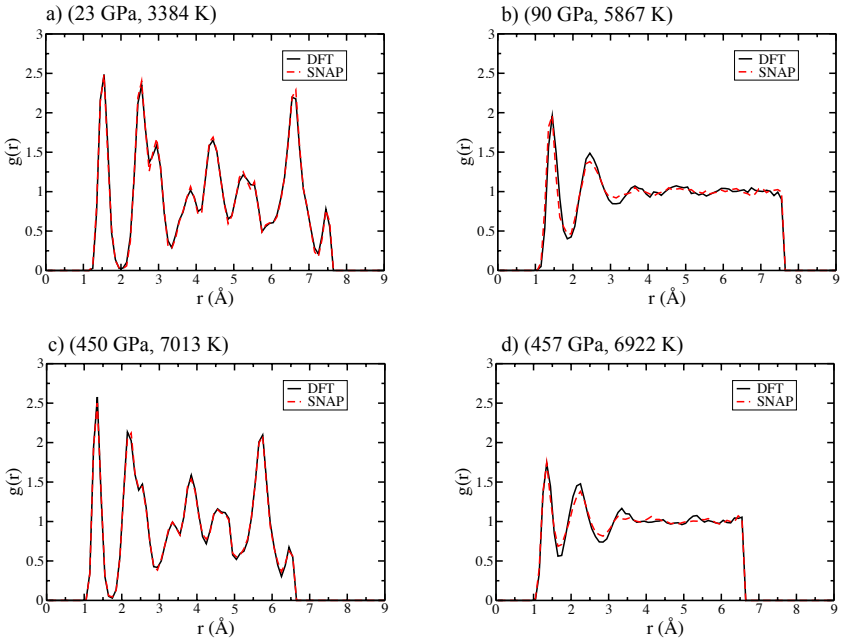

FIGURE 3. Radial distribution functions of diamond and liquid carbon calculated by SNAP and compared to DFT for (a) diamond at (23 GPa, 3884 K); (b) liquid carbon at (90 GPa, 5867 K); (c) diamond at (450 GPa, 7013 K); (d) liquid carbon at (457 GPa, 6922 K).

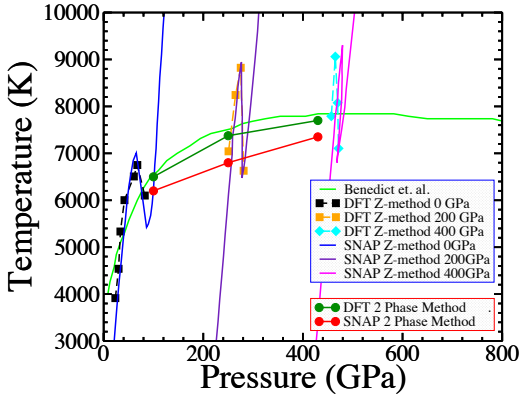

FIGURE 4. Diamond (P, T) melting points calculated by two-phase and Z-methods and compared to our own DFT calculations [15] as well as previous simulations performed by Benedict *et. al* [14].

conditions. This positions carbon SNAP to make DFT accurate simulations at much faster speed. The developed SNAP will be used in large-scale MD simulations of dynamic compression of carbon materials.

ACKNOWLEDGMENTS

The research is supported by the DOE National Nuclear Security Administration (award # DE-NA0003910). Simulations were performed using the DOE leadership HPC supercomputers: OLCF Summit at ORNL (ASCR ALCC award), Cori at NERSC(High-Impact Science at Scale on Cori award) and USF Research Computing Cluster CIRCE.

REFERENCES

1. I. I. Oleynik, A. C. Landerville, S. V. Zybin, M. L. Elert, and C. T. White, Phys. Rev. B **78** (2008).
2. R. Perriot, Y. Lin, V. V. Zhakhovsky, N. Pineau, J. H. Los, J.-B. Maillet, L. Soulard, C. T. White, and I. I. Oleynik, AIP Conference Proceedings **1426**, 1175–1178 (2012).
3. R. Perriot, X. Gu, Y. Lin, V. Zhakhovsky, and I. I. Oleynik, Phys. Rev. B **88**, 64101 (2013).
4. Y. Lin, R. Perriot, V. V. Zhakhovsky, X. Gu, C. T. White, and I. I. Oleynik, AIP Conference Proceedings **1426**, 1171–1174 (2012).
5. A. P. Bartók, M. C. Payne, R. Kondor, and G. Csányi, Phys. Rev. Lett. **104**, 136403 (2010).
6. A. P. Bartók, J. Kermode, N. Bernstein, and G. Csányi, Phys. Rev. X **8**, 41048 (2018).
7. A. P. Thompson, L. P. Swiler, C. R. Trott, S. M. Foiles, and G. J. Tucker, Journal of Computational Physics **285**, 316–330 (2015).
8. M. A. Wood and A. P. Thompson, The Journal of Chemical Physics **148**, 241721 (2018).
9. S. Plimpton, Journal of Computational Physics **117**, 1–19 (1995).
10. A. R. Oganov and C. W. Glass, The Journal of Chemical Physics **124**, 244704 (2006).
11. C. W. Glass, A. R. Oganov, and N. Hansen, Computer Physics Communications **175**, 713–720 (2006).
12. A. O. Lyakhov, A. R. Oganov, and M. Valle, Computer Physics Communications **181**, 1623–1632 (2010).
13. G. Kresse and J. Furthmüller, Computational Materials Science **6**, 15–50 (1996).
14. A. A. Correa, L. X. Benedict, D. A. Young, E. Schwegler, and S. A. Bonev, Phys. Rev. B **78**, 24101 (2008).
15. K. Nguyen-Cong, W. Ashley, J. Willman, A. Belonoshko, and I. I. Oleynik, SCCM Conference Proceedings (2019), In Review.